JOURNAL OF MATERIALS SCIENCE 29 (1994) 6320–6328

# The influence of preceramic binders on the microstructural development of silicon nitride

S. T. SCHWAB, C. R. BLANCHARD, R. C. GRAEF
*Department of Materials Sciences, Southwest Research Institute, San Antonio, Texas, 78228-0510, USA*

A number of polymeric precursors to silicon nitride were prepared and evaluated as binders in cold pressing/pressureless sintering operations. These polymers exhibited ceramic yields in excess of 75% by weight, and powder compacts made using them as binders displayed improved green handling properties. Compacts pyrolysed at 800 °C exhibited unusual microstructures, including the development of whiskers *in situ*. Based on microstructural observation, compacts sintered under pressureless conditions appeared to show enhanced densification relative to those processed without preceramic binders. Preceramic binders appeared to enhance the formation of β-$Si_3N_4$ and may enhance densification of compacts sintered under pressureless conditions.

## 1. Introduction

Advanced ceramics offer unique combinations of mechanical and electro-optical properties and they are finding increased use in high-technology applications [1]. Current techniques of advanced ceramic-component fabrication are based on pressureless green-body consolidation in which voids often remain in the final microstructure. These voids have deleterious effects on the structural properties of the ceramic. Some of this residual porosity is generated when the organic binder which is used to consolidate the ceramic powder is burned off [2, 3]. One approach to minimizing void formation is the substitution of the traditional fugitive binder with an organometallic polymer (preceramic polymer) which will decompose into a predetermined ceramic when fired [4, 5, 6]. The void space normally induced during organic binder burn-out would be replaced by a polymer-derived ceramic [4, 5, 6].

Silicon nitride ($Si_3N_4$) is a ceramic material which is in great demand for its superior high-temperature properties and its excellent strength-to-weight ratio [7]. Unfortunately, like other covalent materials, silicon nitride is difficult to sinter because of its low self-diffusivity [8]. Densification can be achieved without an applied pressure if sintering aids are used; however, the presence of these glassy materials in the ceramic seriously detracts from the material's high-temperature strength [9]. Since components made of graphite or carbon (also covalent species) are successfully fabricated with polymeric precursors, we proposed the development of preceramic polymers for use as binders and the evaluation of their potential for facilitating the pressureless densification of silicon-nitride compacts.

Although the Ceramic Research Association demonstrated the utility of organometallics in the chemical vapour deposition (CVD) of ceramics in the early 1960s [10, 11], it was not until the successful development of polymeric precursors to silicon carbide [12–14], and the commercial success of the Nicalon fibres made from them, that the investigation of polymeric precursors to silicon nitride and other advanced ceramics became widespread. Reviews of preceramic polymers in general [4–6] and of polymeric precursors to silicon nitride (polysilazanes) have recently been published [15].

Seminal work in the synthesis of polymeric precursors to silicon nitride has been performed by researchers at the Massachusetts Institute of Technology (MIT). D. Seyferth and co-workers have developed an elegant synthesis of polymers which decompose in high yields into $Si_3N_4$/SiC mixtures or into silicon oxynitride, depending on the chemistry of the specific precursor and on the pyrolysis conditions [16]. Although they have reported that their materials function well as binders in powder-processing operations, few details of their studies have appeared, and no discussion of the related microstructures has been presented. A group at the Stanford Research Institute (SRI) has reported the synthesis of polysilazanes through transition-metal-catalysed reactions [15], and it has performed preliminary evaluations of their performance as binders [17, 18]. Although sintering aids were also present, the SRI study presents evidence suggesting that the polymer-derived material assists densification [17, 18].

To the best of our knowledge, a description of the microstructures resulting from the use of polysilazane binders in the absence of sintering aids has yet to appear. We have performed such evaluations with three relatively similar polysilazane binders, and have found that the microstructures resulting from their use vary dramatically with subtle changes in the polymer chemistry.



0022–2461 

## 2. Experimental procedure

### 2.1. General

Unless stated otherwise, all manipulations were carried out in the absence of air and moisture on an inert atmosphere/vacuum manifold system or in a drybox (Vacuum Atmospheres HE-43-2 with HE-493 Dri-train) using synthetic inorganic techniques [19, 20]. All solvents were freshly distilled from the appropriate drying agents [21] and they were thoroughly degassed before use. Chlorosilanes were purchased from Petrarch Systems (Bristol, PA., now a division of Hüls), and they were distilled from magnesium prior to use. Anhydrous ammonia (99.99%) was purchased from Liquid Carbonic (San Antonio, TX) and used as-received. Butyl amines were purchased from Aldrich (Milwaukee, WI) and they were distilled from potassium prior to use. Dichlorosilane and trichlorosilane were purchased from Petrarch (now Hüls), and they were purified by trap-to-trap distillation prior to use. Elemental analyses were performed by Galbraith Laboratories (Knoxville, TN). Silicon-nitride powder (grade LC12 $\alpha$-$Si_3N_4$, 0.55 μm average particle size) was purchased from Hermann C. Starck (New York, NY). This powder was stored at a 0% relative humidity and then dried under vacuum before use.

Fourier transform infrared (FTIR) spectra were recorded using a Bio-Rad Digilab Model FTS-15E/D FTIR spectrometer equipped with a Bio-Rad Digilab 3240 data system. Nuclear magnetic resonance (NMR) studies were performed on a Jeol FX-90Q spectrometer operating at 90 MHz. NMR spectra were recorded in deuterobenzene ($C_6D_6$), or other suitable solvents, at ambient temperature and they were referenced to $Me_4Si$ ($\delta$ 0.0). Thermogravimetric analysis (TGA) was performed on a Perkin-Elmer TGS-2, equipped with a system 7/4 controller, under flowing argon. Polymer densities were determined on an inert-gas pycnometer. Pyrolyses below 1000 °C were performed in a Pereny Model MT30K4.102 tube furnace in a fused-silicon-carbide tube under flowing nitrogen. Pressureless sintering operations were performed in a Centorr Associates, Inc. Hot Press (Model # HP-9 × 8-G-G-06A5-A-23) with an Ircon Modline (Type R-99C10) thermal controller. Uniaxial cold-pressing operations were carried out on an Owatonna Tool Company (OTC) 55 ton hydraulic shop press in hardened tool-steel dies lubricated with a thin film of oleic acid.

### 2.2. Polymer synthesis

*N-tert*-butyl hydropolysilazane (1). Dichlorosilane ($H_2SiCl_2$, 49 mL, 0.6 mol) and trichlorosilane ($HSiCl_3$, 20 mL, 0.2 mol) were added to tetrahydrofuran (THF, 1.6 L) at 0 °C. Ammonia ($NH_3$, excess) and *t*-butyl amine ($Bu^tNH_2$, 20 mL, 0.2 mol) were added simultaneously over a period of 1 h, with the ammonia addition continuing for an additional hour. After warming to room temperature, the solution was stirred (4 h), and then heated to reflux under a water-cooled condenser (1.5 h). After cooling to room temperature and settling, the solution was filtered. The majority of the solvent was removed by distillation at ambient pressure under nitrogen. The remaining volatiles were removed *in vacuo* at room temperature to yield a stiff, waxy solid.

*N-n*-butyl hydropolysilazane (2). Dichlorosilane ($H_2SiCl_2$, 79 mL, 0.6 mol) and trichlorosilane ($HSiCl_3$, 30 mL, 0.3 mol) were added to THF (1.6 L) at 0 °C. Ammonia ($NH_3$, excess) and *n*-butyl amine ($Bu^nNH_2$, 30 mL, 0.3 mol) were added simultaneously over a period of 30 min with the ammonia addition continuing for an additional hour. After warming to room temperature, the solution was stirred (12 h) and then heated to reflux under a water cooled condenser (2 h). After cooling to room temperature and settling, the solution was filtered. The precipitate was washed (with 0.25 L THF) and the washings were combined with the filtrate. The majority of the solvent was removed by distillation at ambient pressure under nitrogen. The remaining volatiles were removed *in vacuo* at room temperature to yield a viscous oil.

Perhydropolysilazane (3). Dichlorosilane ($H_2SiCl_2$, 105 mL, 1.21 mol) and trichlorosilane ($HSiCl_3$, 69 mL, 0.69 mol) were added to THF (3 L) at 0 °C. Ammonia ($NH_3$, excess) was added to the reaction mixture by first saturating the solution and then continuing slow addition overnight. The solution was heated to reflux under a dry-ice-cooled ( − 78 °C) condenser (3 h) and then heated to reflux under a water-cooled condenser. After cooling to room temperature and settling, the solution was filtered. The precipitate was washed (0.5 L THF) and the washings were combined with the filtrate. The majority of the solvent was removed by distillation at ambient pressure under nitrogen. The remaining volatiles were removed *in vacuo* at room temperature to yield a clear oil. After standing at ambient temperature for ca. 12 h, the oil was observed to have transformed into a clear solid. Addition of THF was accompanied by a loud popping sound, but no gas evolution was observed. After ca. 400 mL of THF had been added to the solid, a suspension formed. Removal of the THF *in vacuo* yielded the polymer as a white, free-flowing powder.

### 2.3. Material processing and characterization

Sufficient preceramic polymer was added to a suspension of $Si_3N_4$ powder in THF to form a 25% by weight polymer/powder moulding mixture. This slurry was sonicated (ca. 10 min) to facilitate mixing and then it was heated to reflux overnight. Sonication (ca. 10 min) was repeated after the slurry had cooled to room temperature, and the solvent was removed *in vacuo* to yield the moulding mixture as a grey/white free-flowing powder. (Grinding of the mixture with a mortar and pestle was not required.) Billets were obtained by uniaxially pressing the mixture at 30 000 p.s.i. Powders were processed in the same manner in the absence of a binder to provide a control. Selected samples remained in the green state for baseline comparison purposes, while the remaining samples were either pyrolysed in a tube furnace in flowing nitrogen at 800 °C or they were pyrolysed and pressureless sintered at 1820 °C for 5 h following the

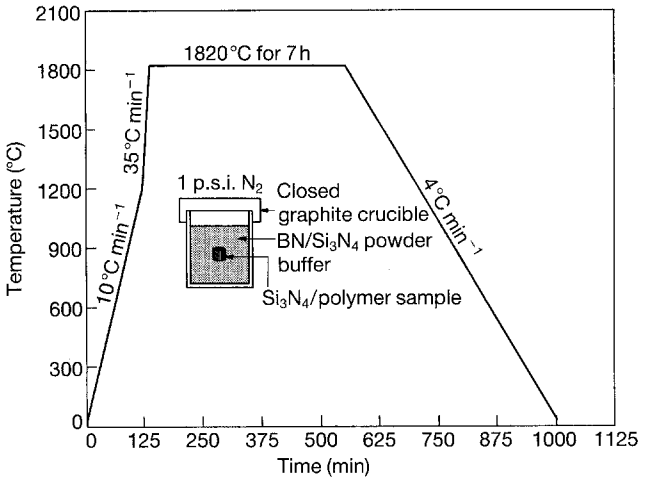


*Figure 1* A schematic diagram showing the pressureless-sintering schedule and the powder-buffer configuration.

sintering schedule shown in Fig. 1. Pressureless sintering operations were carried out under a nitrogen atmosphere with the samples packed in a powder-bed buffer system (50 wt % BN in $Si_3N_4$) enclosed in a graphite crucible to prevent degradation of the $Si_3N_4$ [7].

In general, chemical characterization of the polymers consisted of TGA, FTIR, and NMR analyses. (In one case, the polymer was not sufficiently soluble in the available deuterated solvents to allow NMR analysis.) The composition of the polymer-derived ceramic was generated from the elemental analysis of the chars. Briefly, the weight percentages of the elements were converted into molar percentages and each element was consumed in proportion to the stoichiometry of the likely ceramic constituents (for example, $3Si + 4N = Si_3N_4$, $Si + C = SiC$, etc.). Elements present in excess of the ceramic stoichiometries were considered to be unbound, or "free".

Three preceramic polymers (*N-tert*-butyl hydridopolysilazane (1), *N-n*-butyl hydridopolysilazane (2), and perhydridopolysilazane (3)) and a control group containing no additives (control) were fully processed and characterized. The bulk densities of the green compacts and the pyrolysed compacts were determined by measuring and weighing the samples, while the densities of the sintered materials were determined by Archimedean immersion. (The sintered compacts were inadvertently fractured before the bulk-density measurements were taken.) Microstructural evaluation was recorded by scanning electron microscopy (SEM) analysis of the fracture surfaces of each compact at the green, pyrolysed and sintered stage. The crystalline phases present were determined from the X-ray powder diffraction patterns of ground samples taken from each stage of processing.

## 3. Results and discussion

### 3.1. Properties of the binders and the compacts

There are a number of approaches to the design of preceramic polymers [22]. Because only hydrogen must be removed, perhydropolysilazanes would, in theory, produce the largest amount of ceramic per unit of polymer; however, perhydropolysilazanes are prone to thermal cross-linking, which rapidly produces new intractable materials [23]. Substitution with alkyl groups inhibits this cross-linking process, but it can also introduce carbon to the derived ceramic [16–18]. While a certain amount of carbon can be used to react with the silica ($SiO_2$) present on the surface of the starting powders, an excess of carbon can inhibit densification and it detracts from stability against oxidation [24]. We postulated that partial substitution with bulky alkyl groups would inhibit the cross-linking process while introducing a minimum of carbon to the derived ceramic – particularly if the alkyl groups were prone to the facile β-hydride transfer/alkene elimination process [25]. To explore this possibility, two *N*-substituted hydridopolysilazanes (*tert*-butyl (1) and *n*-butyl (2)) were synthesized and evaluated against a perhydropolysilazane (3). The spectral characteristics of these polymers are presented in Table I, while their performance in compression moulding is outlined in Table II.

Green compacts made with polymers 1 and 2 exhibited good mechanical integrity, in that they did not crumble when handled and they were difficult to break by hand. Green compacts made with polymer 3 tended to crumble, but they were superior to the control compacts nonetheless. With all three binders, the apparent strength of the green compacts appeared to increase when they were stored under an inert atmosphere at room temperature. This apparent strength increase was likely to be a result of thermally induced cross-linking, which would have converted part of the two-dimensional polymer matrix into a stiff three-dimensional network.

### 3.2. Microstructures and crystalline phases

To evaluate the performance during sintering, both the binders and the compacts made with them were subjected to heat treatments. Because the effluent gases generated during pyrolysis were found to be very reactive, the compacts were first pyrolysed at 800 °C under flowing nitrogen in a tube furnace. A TGA of the binders indicated that the weight loss was essentially complete at this temperature. Following pyrolysis, the compacts were heated to 1820 °C under nitrogen in a graphite retort packed with a 50 wt % mixture of boron-nitride and silicon-nitride powder (see Fig. 1). This buffer mixture was used to prevent the reported [7] decomposition of the silicon-nitride powders above 1500 °C.

Table III presents the densities of the compacts made with the preceramic polymers (1, 2, and 3; 25% by weight) and the binder-free control at the various stages of processing. The green-body densities are reported relative to both the theoretical density of pure $Si_3N_4$ (3.2 $g\,cm^{-3}$) and the theoretical density of a void-free, 25% by weight, mixture of $Si_3N_4$ and polymer ($\sim 1\ g\,cm^{-3}$). As it was assumed that heating to 800 °C was sufficient to essentially complete the conversion of polymer to ceramic, the densities of the pyrolysed and sintered bodies are reported relative to pure $Si_3N_4$ only.

TABLE I The spectral properties of *N-tert*-butylhydropolysilazane (1), *N-n*-butylhydropolysilazane (2) and perhydropolysilazane (3)

| Polymer | $^1$H NMR[a] (p.p.m.) | FTIR[b] ($cm^{-1}$) |
|---|---|---|
| 1 | 0.35(s), 0.5(s), 0.9–1.6(m), 3.55–3.75(t), 4.5–5.5(br m) | 3375m, 2980w, 2880w, 2175s, 1550w, 1190s, 1025s, 940s, 725m |
| 2 | 0.35(s), 0.8–2.0(br d), 2.5–3.3(br s), 4.5–5.9(br d) | 3630w, 3525w, 3480w, 3380w, 2965m, 2940m, 2877w, 2180m, 1705w, 1585w, 1550w, 1475w, 1435w, 1405w, 1390w, 1170s, 1080s, 1035s, 965s, 850s, 760s, 725s |
| 3 | Insufficiently soluble | 3740w, 3660w, 3480w, 3370m, 3090w, 2970w, 2160s, 1545w, 1265w, 1180m, 835s, 715s |

[a] Values expressed in parts per million (p.p.m.), s = singlet, d = doublet, t = triplet, m = multiplet and br = broad.
[b] Values expressed in wavenumbers ($cm^{-1}$), s = strong, m = medium and w = weak absorption.

TABLE II A summary of a compression moulding study of polymer binders 1, 2, and 3 (the moulding mixtures were 25% by weight polymer)

| Polymer | Form | Ceramic yield[a] (1000 °C) | Char composition[b] | Green compact quality |
|---|---|---|---|---|
| 1 | Wax | 89 | 92.7 $Si_3N_4$<br>1.4 SiC<br>3.1 $SiO_2$<br>2.8 free Si | Excellent |
| 2 | Viscous oil | 79 | 90.2 $Si_3N_4$<br>9.6 SiC<br>0.2 free Carbon | Excellent |
| 3 | Powder | 92 | 93.6 $Si_3N_4$<br>0.5 SiC<br>2.7 $SiO_2$<br>3.2 free Si | Fair<br>(somewhat crumbly) |

[a] By TGA.
[b] Values expressed in percentages by weight, determined from elemental analysis.

TABLE III Compact densities (percentage of theoretical density)

| | Green body[a] | Green body[b] | Pyrolysed body | Sintered body |
|---|---|---|---|---|
| Control | 62.2 | – | 61.9 | 95.7 |
| 1 | 61.8 | 72.3 | 69.3 | 92.0 |
| 2 | 70.0 | 81.7 | 72.8 | 95.6 |
| 3 | 50.6 | 59.1 | 52.2 | 82.4 |

[a] Based on the theoretical density of silicon nitride (3.2 g $cm^{-3}$).
[b] Based on the theoretical density of a weighted average of silicon nitride and polymer (the polymer density was assumed to be ~1 g $cm^{-3}$).

It may be inferred from the green-body densities that polymer 2 appears to have had a beneficial effect on the moulding-mixture compaction, while polymer 3 had a somewhat deleterious effect and polymer 1 had essentially no effect. The polymers' influence on the green-body density appears to be a function of their viscosity. Polymer 2, isolated as a thick oil, is the least viscous of these three binders, and its presence may have added some lubricity to aid in the moulding process. Polymer 3, isolated as a powder, is the most viscous of the three. Individual granules of polymer 3 were somewhat sticky or tacky, and its presence in the mixture could well have inhibited particle packing. Polymer 1, isolated as a wax, is of intermediate viscosity. While polymer 1 is somewhat sticky, it flows under applied pressure. The state of polymer 1 appears to have had little effect during compression moulding as it yielded a compact with essentially the same density as that obtained with the powder alone.

Following pyrolysis, the density of the control specimen remained essentially unchanged, while the densities of the compacts containing preceramics decreased substantially relative to the theoretical value which includes the starting density. This decrease in the density probably results from the conversion of the binder to an amorphous covalent ceramic [26]. While the nature of the amorphous covalent ceramic produced from polysilazanes is under study [27], it appears to exhibit a defect-rich structure with a density well below that of crystalline $Si_3N_4$. Regardless of the exact nature of the polymer-derived ceramic at this stage of processing, the relative order of each compact is unchanged from the green state. The compact containing polymer 2 exhibits the highest density and the compact containing polymer 3 exhibits the lowest; the compact containing polymer 1 falls between. It is of interest that the pyrolysed density of the polymer 1 compact dropped a mere 3% from its green density (polymer included) while the densities of the polymer 2 and polymer 3 compacts dropped nearly 9% and 7%, respectively. The density of the polymer 1 compact also increased substantially relative to the control.

The compacts were inadvertently fractured before the sintered densities were measured. The values presented in Table III for the sintered densities were

determined using Archimedean immersion, and they appear to be substantially higher than would have been expected on the basis of the green and pyrolysed densities. It seems likely that the compacts contained a substantial amount of closed porosity which was not accounted for in the immersion experiments. Despite the surprisingly high measured density values, the error is likely to be the same for each, so the relative ranking of each material should be the same, regardless of the measurement method.

While the relative order of the polymer-containing compacts did not change (polymer 2 was the best, and polymer 3 was the worst, with polymer 1 being intermediate), they all had a lower density than the control. While the polymer 2 compact exhibited green and pyrolysed densities substantially greater than that of the control, its sintered density was essentially the same as the control, with the other compacts having somewhat smaller values.

The ceramic products of polymer 1 and polymer 3 (Table II) contained substantial amounts of elemental silicon and $SiO_2$, while the products of polymer 2 were essentially all $Si_3N_4$ and SiC. It is possible that, rather than reacting with nitrogen (nitriding), any elemental silicon and/or silica present volatilized from the compact, leaving void space.

To determine what crystallographic phase changes had taken place during pyrolysis and sintering, samples from each processing step were examined by powder X-ray diffraction; the results are presented in Table IV. In accordance with the product literature, the starting powder was composed primarily of $\alpha$-$Si_3N_4$. While pyrolysis did not induce any phase transformation in the control, sintering induced the appearance of $\beta$-$Si_3N_4$ as a minor constituent. The compacts made with the preceramic binders also exhibited only $\alpha$-$Si_3N_4$ in the green and in the pyrolysed state; however, upon sintering, the result was reversed, with $\beta$-$Si_3N_4$ appearing as the major and $\alpha$-$Si_3N_4$ as the minor constituent.

The $\alpha$-$Si_3N_4$ to $\beta$-$Si_3N_4$ phase transformation is not fully understood, but it is believed to be promoted by the presence of a liquid phase [7, 28]. As reflected in Table II, pyrolysis of the preceramic binders produces silica ($SiO_2$, melting point (m.p.) ca. 1600–1725 °C), free silicon (Si, m.p. 1410 °C), free carbon, and silicon carbide in addition to silicon nitride. Because it did not diffract X-rays and it was assumed to be amorphous, the char composition was derived from an elemental analysis. As there is no way to verify that the listed elements are indeed bound in the indicated materials, silicon, which has been shown to promote the $\alpha$-$Si_3N_4$ to $\beta$-$Si_3N_4$ phase transformation [29], may be present in greater amounts than are implied in Table II. If a liquid phase formed from the silica and/or the silicon produced during pyrolysis, it could have enabled a significant amount of $\alpha$ to $\beta$ phase transformation to occur, which would account for the increased amount of $\beta$-$Si_3N_4$ observed in the samples containing polymer-derived material.

TABLE IV X-ray-diffraction results

| | Green body | Pyrolysed body | Sintered body |
|---|---|---|---|
| Control | | | |
| Major constituent | $\alpha$-$Si_3N_4$ | $\alpha$-$Si_3N_4$ | $\alpha$-$Si_3N_4$ |
| Minor constituent | – | – | $\beta$-$Si_3N_4$ |
| Polymer 1 | | | |
| Major constituent | $\alpha$-$Si_3N_4$ | $\alpha$-$Si_3N_4$ | $\beta$-$Si_3N_4$ |
| Minor constituent | – | – | $\alpha$-$Si_3N_4$ |
| Polymer 2 | | | |
| Major constituent | $\alpha$-$Si_3N_4$ | $\alpha$-$Si_3N_4$ | $\beta$-$Si_3N_4$ |
| Minor constituent | – | – | $\alpha$-$Si_3N_4$ |
| Polymer 3 | | | |
| Major constituent | $\alpha$-$Si_3N_4$ | $\alpha$-$Si_3N_4$ | $\beta$-$Si_3N_4$ |
| Minor constituent | – | – | $\alpha$-$Si_3N_4$ |

The $\alpha$–$\beta$ transformation is a key step in the densification of $Si_3N_4$. The apparent enhancement of this transformation in the polymer-containing compacts suggests that, despite the measured densities, preceramic binders can enhance densification of $Si_3N_4$ under pressureless conditions.

The microstructural evolution of the compacts during processing is depicted in the fracture surfaces illustrated in Figs 2–5. It can be seen that subtle changes in the polymer chemistry appear to have induced dramatic microstructural changes as the processing progressed. The green bodies of the compacts made with polymer 1 (Fig. 3a) and polymer 2 (Fig. 4a) exhibit microstructures which are indicative of two extremes of binder addition, while the sample containing polymer 3 (Fig. 5a) more closely resembles the control (Fig. 2a). From the green densities listed in Table III, it would have been expected that polymer 2 and polymer 3 would have exhibited the polymer-influenced microstructures and that polymer 1 would have more closely resemble the control. The low viscosity and high solubility (in THF during moulding-mixture preparation) of polymer 2 promoted its homogeneous distribution through the microstructure, as reflected in Fig. 4a. In contrast, the lower THF solubility and higher viscosity of polymer 1 have hindered its even distribution in the microstructure and produced regions devoid of powder. Although segregation during sonication may also explain the inhomogeneous microstructure, the density of each preceramic was essentially the same, and the processing conditions were also identical. If segregation was occurring, inhomogeneous microstructures would have been expected for each compact, but they were only observed in the compacts containing polymer 1. As polymer 3 was isolated as a powder, it is not surprising that the microstructure of the sample containing it is similar to that of the control. It seems plausible that during the slurry-mixing process, the action of the abrasive $Si_3N_4$ powder would have ground the polymer into very fine particulates, which would have been evenly distributed through the microstructure as in any traditional powder additive.

Pyrolysis induced a dramatic differentiation in the microstructures of the compacts containing the preceramic polymers. While the compact containing polymer 1 (Fig. 3b) changed little during pyrolysis, the compacts containing polymer 2 and polymer 3 underwent major microstructural changes. In the compact containing polymer 2, pyrolysis induced the formation

of a whisker-enriched microstructure, as seen in Fig. 4b and c. This *in-situ* whisker formation was not observed in any of the other samples. While *in-situ* growth of SiC whiskers has been reported by others [30–32], to the best of our knowledge this is the first observation of *in-situ* growth of $Si_3N_4$ whiskers. While the whisker morphology is generally associated with $\beta$-$Si_3N_4$, as seen in Table IV only $\alpha$-$Si_3N_4$ was detected in this sample. As this whisker enrichment was

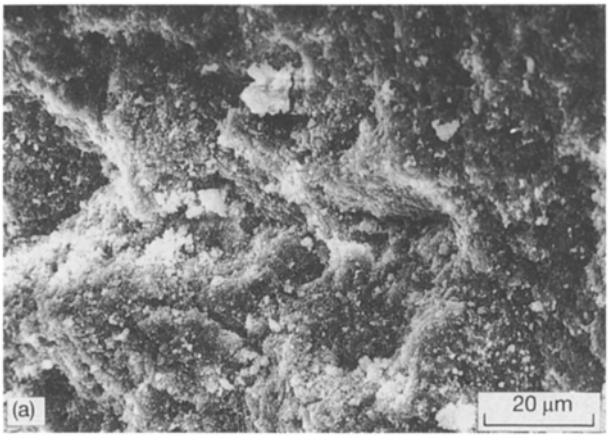


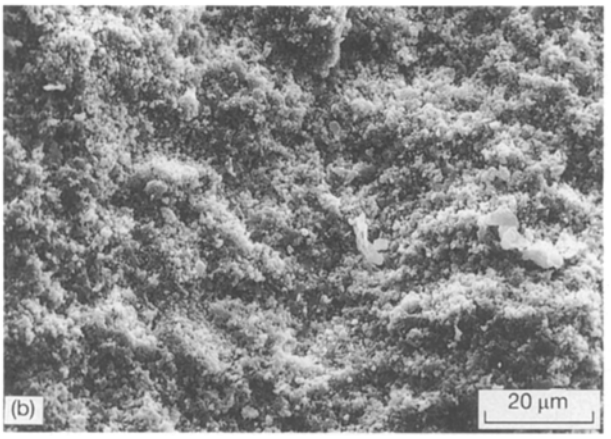


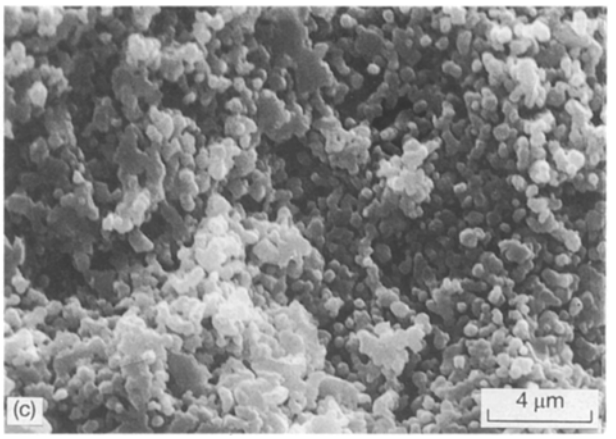


*Figure 2* The fracture surfaces of the control compact, processed with no binder additive: (a) in the green state, (b) after pressureless sintering at 1820 °C, and (c) at a higher magnification of the sintered microstructure.

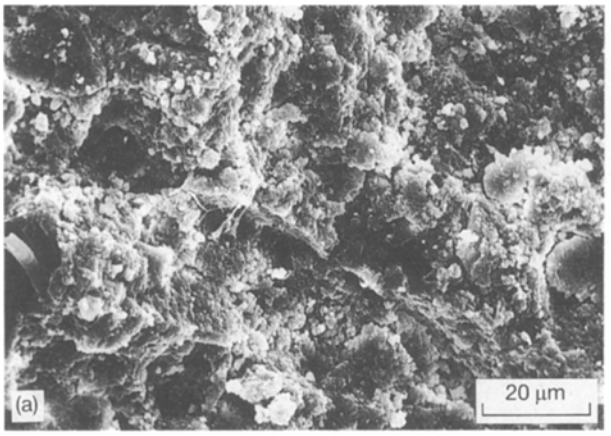


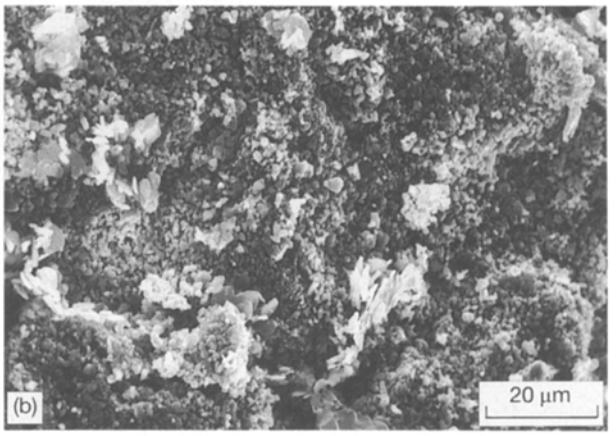


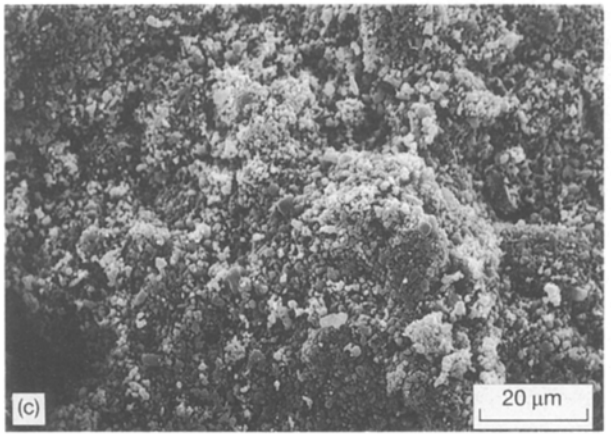


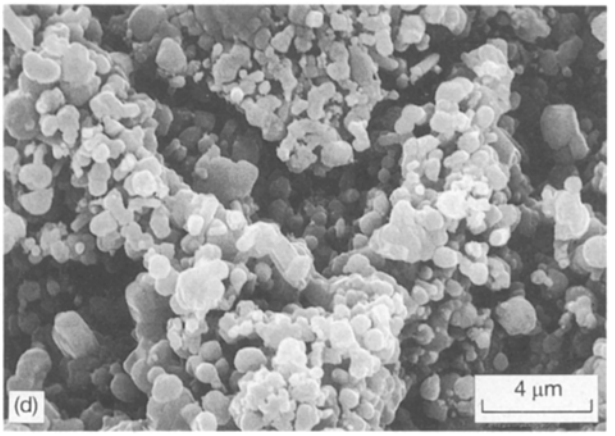


*Figure 3* The fracture surfaces of the compact processed with the polymer 1 binder: (a) in the green state, (b) and (c) after pressureless sintering at 1820 °C, and (d) at a higher magnification of the sintered microstructure.

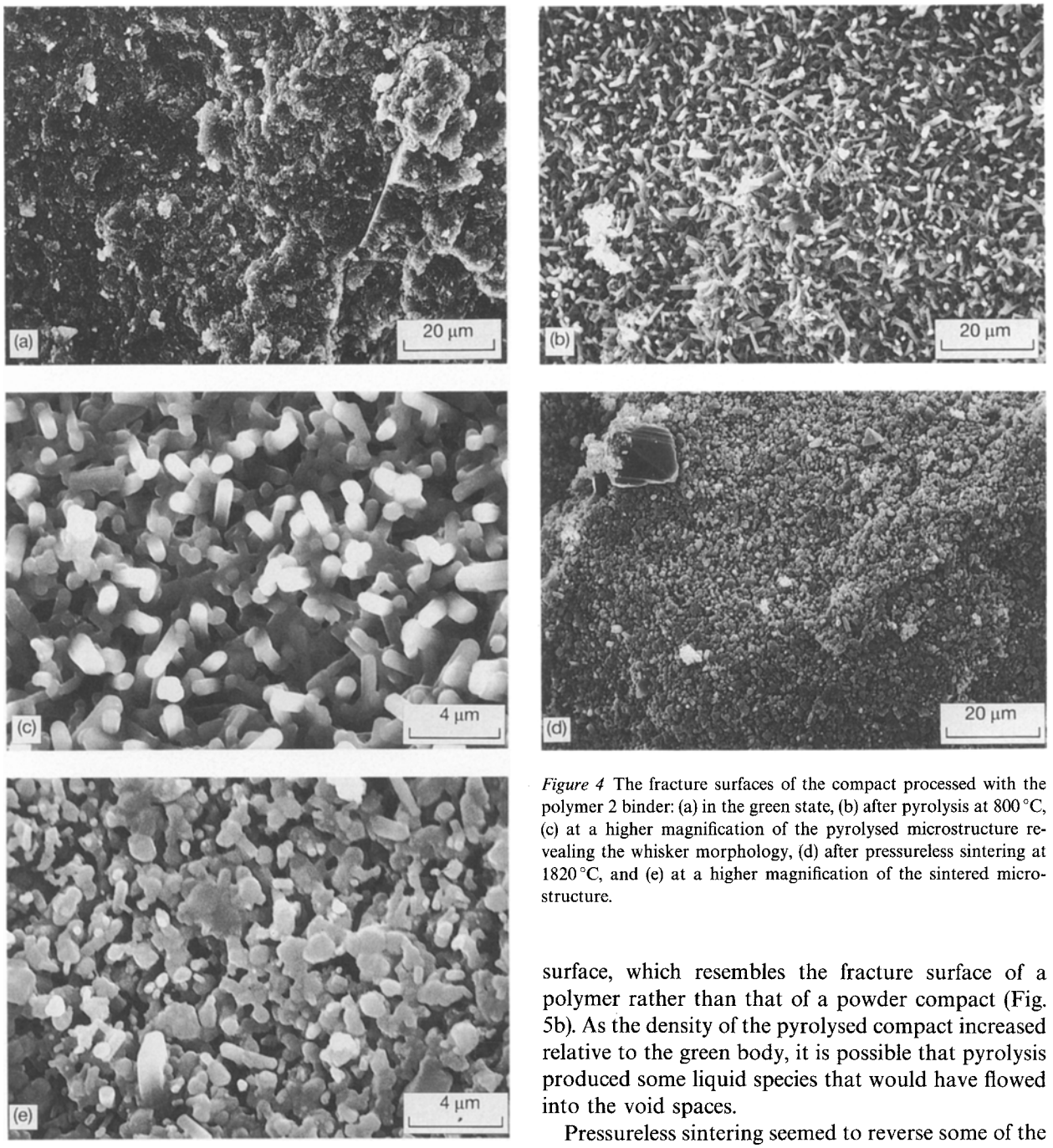


*Figure 4* The fracture surfaces of the compact processed with the polymer 2 binder: (a) in the green state, (b) after pyrolysis at 800 °C, (c) at a higher magnification of the pyrolysed microstructure revealing the whisker morphology, (d) after pressureless sintering at 1820 °C, and (e) at a higher magnification of the sintered microstructure.

limited to the samples containing polymer 2, some specific aspect of this material's pyrolysis must be responsible, but one can only speculate as to what that aspect may be. The temperature at which the events took place (800 °C) is much lower than is usually observed in microstructural developments of this type; nonetheless, β-$Si_3N_4$ has been observed to form from amorphous materials in Si–C–N systems at temperatures as low as 900 °C [33]. Also, a similar $Si_3N_4$ whisker morphology was observed previously [34], but the whiskers were identified as elongated β-grains. Perhaps a similar phenomenon is occurring here, with the formation of α-$Si_3N_4$ whiskers being driven by the template effect of the powder.

In the sample containing polymer 3, the fracture surface of the green body (Fig. 5a) appears rough and grainy, as expected for a compacted powder. Following pyrolysis, powder is no longer evident in the fracture surface, which resembles the fracture surface of a polymer rather than that of a powder compact (Fig. 5b). As the density of the pyrolysed compact increased relative to the green body, it is possible that pyrolysis produced some liquid species that would have flowed into the void spaces.

Pressureless sintering seemed to reverse some of the dramatic microstructural developments which are observed in the pyrolysed samples. In the control sample (Fig. 2b and c), essentially no sintering has taken place, as indicated by the small particle size and the lack of elongated β-$Si_3N_4$-type grains. Little α-$Si_3N_4$ to β-$Si_3N_4$ conversion, which is thought to be a requirement for sintering [7], appears to have taken place, as reflected in the X-ray diffraction analysis. In contrast, the samples made with the preceramic polymers are clearly in the initial stages of sintering, as indicated by the particle–particle necking, the grain coalescence and growth, and the formation of elongated β-$Si_3N_4$ grains observed in the micrographs (polymer 1, Fig. 3c and d; polymer 2, Fig. 4d and e; and polymer 3, Fig. 5c and d). While some elongated β-$Si_3N_4$ grains are observed in the microstructure of the compact containing polymer 2, the dramatic whisker enrichment observed in the pyrolysed sample has been lost.

Regardless of the microstructures observed in the final ceramic, it is clear that the preceramic polymers

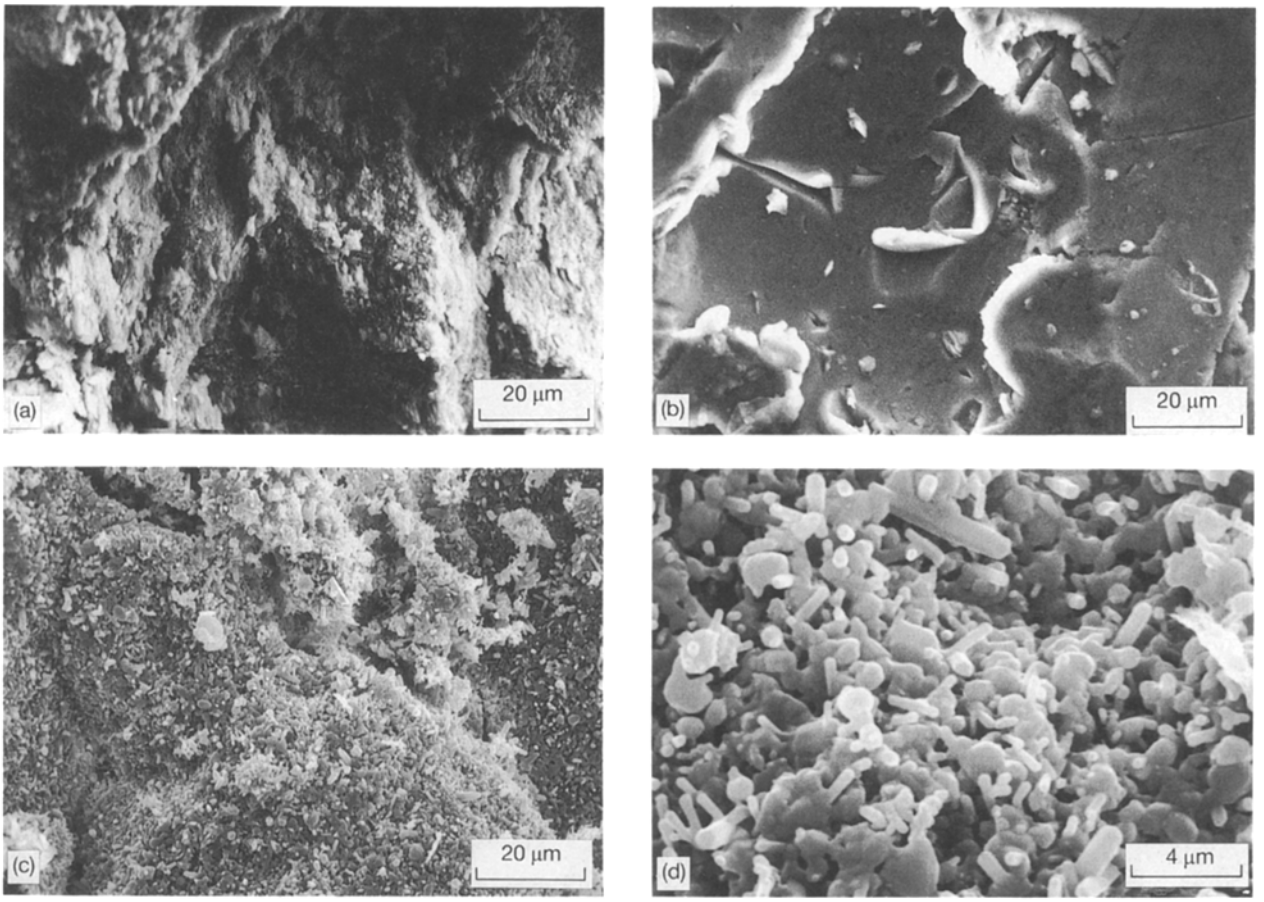


*Figure 5* The fracture surfaces of the compact processed with the polymer 3 binder: (a) in the green state, (b) after pyrolysis at 800 °C, (c) after pressureless sintering at 1820 °C, and (d) at a higher magnification of the sintered microstructure.

and their pyrolysis products have promoted the pressureless sintering of the powder compacts relative to the polymer-free control. In addition, the use of preceramic binders has resulted in compacts exhibiting improved green handling characteristics. While the events associated with the pyrolysis and sintering of the compacts are poorly understood, it is apparent that the incorporation of the preceramic polymers has had a marked and dramatic influence on the microstructural evolution.

## 4. Conclusion

A number of polymers have been synthesized that perform well as binders in cold-pressing operations, and which promote densification of the ceramic during pressureless sintering. The processing of compacts made with preceramic polymers has been shown to be accompanied by unusual microstructural developments, the most dramatic of which was the formation of whiskers *in situ*. The preceramic binders or their pyrolysis products appear to promote the formation of β-$Si_3N_4$, which is generally associated with the densification of $Si_3N_4$. While the measured densities are inconclusive, the accelerated formation of the β-phase suggests that preceramic binders may provide enhanced densification of $Si_3N_4$ powder compacts sintered under pressureless conditions.

## Acknowledgements

Support for this effort was provided by the Southwest Research Institute Internal Research Program and the Air Force Office of Scientific Research under Contract No. F49620-91-C-0045. The United States Government is authorized to reproduce and distribute reprints for governmental purposes notwithstanding any copyright notation hereon. The authors acknowledge with gratitude the technical support of Mr S. Salazar, Mr J. L. Sievert, Mr H. G. Saldana and Ms L. L. Ramon.

## References

1. J. B. WACHTMAN, Jr., W. RHODES, H. K. BOWEN, D. BUCKLEY, E. CROSS, R. J. EAGAN, A. EVANS, G. HAERTLING, J. PANZARINO, D. READEY, R. RICE, G. M. ROSENBLATT, D. GROVES, A. R. HOFFMANN, L. R. McCREIGHT and R. REYWICK, "Research briefings 1985" (National Academy: Washington, DC 1985) pp. 67–71.
2. W. D. KINGERY, H. K. BOWEN and D. R. UHLMANN in "Introduction to ceramics", 2nd Edn (John Wiley, New York, 1976).
3. W. D. KINGERY in "Ceramic fabrication processes" (John Wiley, New York, 1960).
4. K. J. WYNNE, "Transformation of organometallics into common and exotic materials: design and activation", NATO ASI Series E No. 141, edited by R. M. Laine (Martinus Nijhoff, Dordrecht, 1988) pp. 89–96.
5. K. J. WYNNE and R. W. RICE, Wynne, *Ann. Rev. Mater. Sci.* **14** (1984) 297.
6. R. W. RICE, *Amer. Ceram. Soc. Bull.* **62** (1983) 889.
7. G. ZIEGLER, J. HEINRICH and G. WÖTTING, *J. Mater. Sci.* **22** (1987) 3041.
8. O. YEHESKREL, Y. GEFEN and M. TALINKER, *ibid.* **19** (1984) 745.
9. T. HAYAKHI, H. MUNAKATA, H. SUZUKE and H. SAITO, *ibid.* **21** (1986) 3501.

10. P. POPPER, in "Special ceramics 1962", edited by P. Popper (Academic Press, New York, 1963) pp. 137–150.
11. P. G. CHANTRELL and P. POPPER, in "Special ceramics 1964", edited by P. Popper (Academic Press, New York, 1965) pp. 87–103.
12. S. YAJIMA, J. HAYASHI and M. OMORI, *Nature* **261** (1976) 683.
13. S. YAJIMA, M. OMORI, J. HAYASHI, K. OKAMURA, T. MATSUZAWA and C. LIAW, *Chem. Lett.* **563** (1976) 563.
14. S. YAJIMA, Y. HASEGAWA and J. M. IIMURA, *J. Mater. Sci.* **13** (1978) 2569.
15. R. M. LAINE, Y. D. BLUM, D. TSE and R. D. GLASER, "Inorganic and organometallic polymers", edited by M. Zeldin, K. J. Wynne and H. R. Allcock, ACS Symposium Series 360, (American Chemical Society, Washington, DC, 1988) pp. 124–142.
16. D. SEYFERTH, G. H. WISEMAN, J. M. SCHWARK, Y.-F. YU and C. A. POUTASSE, "Inorganic and organometallic polymers", edited by M. Zeldin, K. J. Wynne and H. R. Allcock, ACS Symposium Series 360 (American Chemical Society, Washington, DC, 1988) pp. 143–155.
17. K. B. SCHWARTZ, D. J. ROWCLIFFE and Y. D. BLUM, *Adv. Ceram. Mater.* **3** (1988) 320.
18. K. B. SCHWARTZ and Y. D. BLUM, *Mater. Res. Soc. Symp. Proc.* **121** (1988) 483.
19. D. F. SHRIVER and M. A. DREZDZON in "The manipulation of air-sensitive compounds", 2nd Edn (John Wiley, New York, 1986).
20. A. L. WAYDA and M. Y. DARENSBOURG in "Experimental organometallic chemistry", ACS Symposium Series 357 (American Chemical Society, Washington, DC, 1987).
21. A. J. GORDON and R. A. FORD in "The chemist's companion" (Wiley, New York, 1972).
22. R. H. BANEY, *Chemtech* **18** (December 1988) 738.
23. A. STOCK and K. SOMIESKI, *Ber. dt. Chem. Ges.* **54** (1921) 740.
24. J. R. STRIFE and J. E. SHEEHAN, *Ceram. Bull.* **67** (1988) 369.
25. F. A. COTTON and G. WILKINSON, in "Advanced inorganic chemistry, 4th Edn" (John Wiley, New York, 1980) p. 1120.
26 G. D. SORANU, F. BABONNEAU and J. D. MACKENZIE, *J. Mater. Sci.* **25** (1990) 3886.
27. C. R. BLANCHARD and S. T. SCHWAB, *J. Am. Cer. Soc.* **77** (1994) 1729.
28. M. MITOMO, N. YANG, Y. KISHI and Y. BANDO, *J. Mater. Sci.* **23** (1988) 3413.
29. J. Y. PARK and C. H. KIM, *ibid.* **23** (1988) 3049.
30. H. WANG and G. S. FISCHMAN, *J. Amer. Ceram. Soc.* **74** (1991) 1519.
31. S. YAMADA, S. KIMURA, E. YASUDA, Y. TANABE and Y. ASAMI, *J. Mater. Res.* **3** (1988) 538.
32. R. V. KRISHNA RAO and M. M. GODKHINDI, *J. Mater. Sci.* **27** (1992) 2726.
33. P. E. D. MORGAN, *ibid.* **15** (1980) 791.
34. G. GRESKOVICH and J. H. ROSOLOWSKI, *J. Amer. Cer. Soc.* **59** (1976) 336.

*Received 20 October 1992*
*and accepted 21 February 1994*